Influence of the line characterization on the transient analysis of nonlinearly loaded lossy transmission lines

Influence of the Line Characterization on the Transient Analysis of Nonlinearly Loaded Lossy Transmission Lines

I. Maio, S. Pignari, and F. Canavero

Abstract—**The analysis of nonlinearly terminated lossy transmission lines is addressed in this paper with a modified version of a method belonging to the class of *mixed* techniques, which characterize the line in the frequency domain and solve the nonlinear problem in the time domain via a convolution operation. This formulation is based on voltage wave variables defined in the load sections. The physical meaning of such quantities helps to explain the transient scattering process in the line and allows us to discover the importance (so far often overlooked) of the reference impedance used to define the scattering parameters. The complexity of the transient impulse responses, the efficiency of the algorithms, and the precision of the results are shown to be substantially conditioned by the choice of the reference impedance. The optimum value of the reference impedance depends on the amount of line losses. We show that a low-loss line can be effectively described if its characteristic impedance or the characteristic impedance of the associated LC line is chosen as the reference impedance. Based on the physical interpretation of our formulation, we are able to validate the numerical results, and to demonstrate that, despite claimed differences or improvements, the formulations of several mixed methods are fundamentally equivalent.**

I. Introduction

THE PROBLEM OF signal propagation along transmission lines loaded by nonlinear elements has a central role in the modern technology of signal processing and transmission. Fast digital and analog circuits, at any level of integration, offer a wide choice of examples of single and multiconductor transmission lines connected with nonlinear devices. The decreasing rise time of signal waveforms emphasizes the importance of the propagation effects, and the signal corruption caused by parasitic phenomena as losses and skin effect is now a relevant issue in many applications. On the other hand, the switching operation of nonlinear devices reduces the allowable tolerance to the signal degradation, increasing once more the sensitivity of the system performance to the propagation processes. As a result, in the last years a growing interest has developed for precise and fast (possibly capable of a CAD implementation) analysis methods to forecast the behavior of lossy and dispersive multiconductor lines in nonlinear circuits.

Manuscript received August 26, 1992; revised August 19, 1993. This work was supported by a grant from the Italian Ministry of Scientific Research, and by EEC/Science contract SC1*CT91-0690. This paper was recommended by Associate Editor F.-Y. Chang.

The authors are with the Politecnico di Torino, Dipartimento di Elettronica, I-10129 Torino, Italy.

IEEE Log Number 9216711D.

A full numerical "brute force" solution of the line equations with respect to space and time variables is the most direct approach to the problem (*e.g.*, see [1]). A great advantage of this method is the absence of analytical work, but this translates into a weakness, because the direct numerization of the fundamental equations leaves a little space for a physical interpretation and a deeper insight into the transient process. The consequence is the need for an extensive validation, that guarantees the reliability of the outcome of the numerical procedure. Parallel to all-numerical methods, a great deal of work has been recently devoted to the development of *mixed* approaches that have some remarkable features. These methods exploit the natural formulation of both linear and nonlinear electric systems; in fact, they adopt a frequency domain characterization for the line (which is the basic linear element of the system) and the time domain characteristic equations for the loads (where the nonlinearities are), and combine the two by means of a convolution operation [2]–[11]. Of course, these methods are not free from numerical computations, since the presence of nonlinearities requires the use of numerical solvers. However, a basic feature of this class of methods is that the terms of the solution equations retain an evident physical meaning, so that their interpretation offers a way to check the final results: we use this property to validate our simulations in Section VI. The form of the equations of these mixed methods does not prevent their authors from finding efficient numerical algorithms, that can also be considered for the implementation in a CAD environment. In particular, [2], [6], [12] exploit the generalized method of characteristics and introduce simple line equivalents that do not need an *ad hoc* solver, but can be handled by a standard circuit simulator (*e.g.*, SPICE).

The wide variety of alternatives proposed in the literature on mixed methods, however, can disorient the reader looking for a solution algorithm. All the mixed methods, in fact, have in common many fundamental aspects, but a critical comparison aimed at studying their equivalence and the effect of different parameter choices has never been attempted.

In this paper, we present a critical review of the most important mixed methods proposed in the literature [3]–[11], examining their characterizing element, i.e. the set of transient equations on which they are built. The comparison is made with reference to a new set of transient equations that we propose here. Our new set originates from a modification of the method used in [4], and has the advantage of providing a

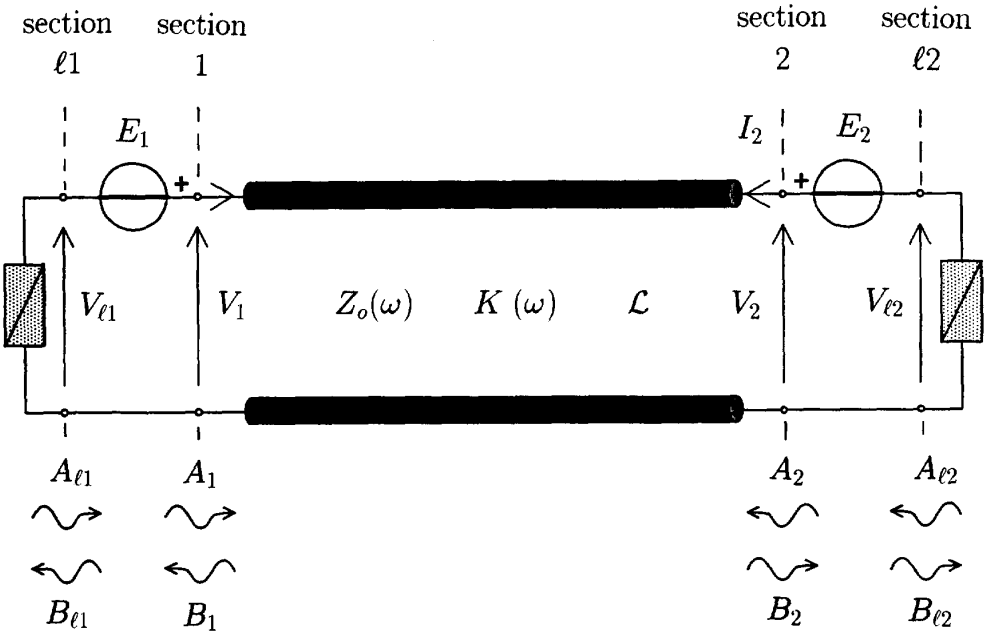

Fig. 1. Nonlinearly loaded scalar transmission line where the voltage waves (A's and B's), relevant for our formulation, are indicated. The voltage sources E_1 and E_2 account for the system excitation, and the other quantities are defined in the text.

deeper physical insight into the transient process. In particular, the physical interpretation of the transients allows us to discuss the influence of the line characterization on the equation final form that reflects on the complexity of the transient problem. We show that the line losses affect the choice of the reference impedance to be used in the definition of the scattering parameters. The consequence is that the optimum solution procedure is influenced by the line type: this is an important new result, since the authors of previous papers often led the readers under the impression that the reference impedance is not a relevant parameter. The ultimate objective of this paper is to present a unified point of view of the mixed methods proposed for the transient analysis of nonlinearly loaded lines, and to offer, through a better physical understanding of the process, a rationale for an efficient application to practical problems.

A summary of the structure of the paper follows. Section II is devoted to the new transient equations, and the influence of the line characterization and losses is discussed in Sections III and IV. The transient equations of the principal mixed methods are thoroughly reviewed in Section V, and the example of Section VI is used to evidence the relevance of our recommendations in a practical case.

Finally, it is worthwhile to clarify the notations that are used in this paper. Lower case letters represent time domain variables and upper case letters indicate their counterparts in the frequency domain, *e.g.*, $x(t) \overset{\mathcal{F}}{\underset{\mathcal{F}^{-1}}{\rightleftharpoons}} X(\omega)$, and $\mathcal{F}$ denotes the Fourier transform operation. Also, the boldface character is used for the collections of elements, and the superscript $\square$ distinguishes matrices from vectors, *i.e.* $\mathbf{a}$ indicates a time-varying vector and $\mathbf{Z}^{\square}$ is a matrix in the frequency domain.

II. Scattering Transient Equations

The problem of analyzing the transient behavior of a transmission line terminated on nonlinear loads is summarized in Fig. 1, where a two-wire line is represented, for simplicity. The extension to multiconductor lines is postponed to the end of this section.

The unknowns of the problem are the voltages $v_1(t)$, $v_2(t)$, and the currents $i_1(t)$, $i_2(t)$ at the line ends. The load networks are represented by Thevenin-like equivalents, whose possible nonlinearity is described by the functions (or operators) $-i_p = g_p(v_{\ell p})$, $p = 1, 2$. The transmission line is characterized by the impedance $Z_o(\omega)$ and the propagation constant $K(\omega)$: the frequency dependence of these functions arises from line losses, and purely dispersive lines, addressed in [5], can be considered as a special case of lossy lines.

Before writing the key expressions of our formulation, we shall review some features of the scattering parameters, that are essential elements for the derivation. We adopt the following form for the relationships between voltage waves and voltages and currents at port p of an electrical network [13]:

$$A_p = \frac{1}{2}(V_p + Z_r I_p)$$
$$B_p = \frac{1}{2}(V_p - Z_r I_p) \tag{1}$$

and

$$V_p = A_p + B_p$$
$$I_p = Y_r(A_p - B_p) \tag{2}$$

where $Z_r(\omega)$ is the reference impedance, Y_r is the corresponding admittance ($Y_r = 1/Z_r$), and the usual factor $1/\sqrt{Z_r}$ in the definition of the wave variables has been dropped here.

The voltage waves at the line ends (see Fig. 1) are related by the scattering equations, whose transient expression becomes

$$\begin{aligned} b_1 &= s_{11r} * a_1 + s_{21r} * a_2 \\ b_2 &= s_{21r} * a_1 + s_{11r} * a_2 \end{aligned} \tag{3}$$

where the symbol $*$ indicates a convolution, and s_{pqr} are the time-domain scattering parameters that, however, are usually defined in the frequency domain, as $S_{pqr} = B_p/A_q$ ($p = 1, 2$; $q = 1, 2$).

In (3), the symmetry of the line is exploited ($s_{11r} = s_{22r}$, $s_{21r} = s_{12r}$). The label r in s_{pqr} reminds that the scattering parameters depend on the reference impedance Z_r selected to define the voltage waves. In fact, s_{21r} (s_{11r}) represents the line transmission (reflection) response to the impulse $a_1 = \delta(t)$, when the line end 2 is closed on the reference impedance, *i.e.* $a_2 = 0$.

Our formulation of the problem is based on the voltage waves defined in the load sections, instead of at the line ends (section ℓp instead of p in Fig. 1.) The relationships between the voltage waves of these two sections are

$$\begin{aligned} a_p &= a_{\ell p} + \frac{1}{2} e_p \\ b_p &= b_{\ell p} + \frac{1}{2} e_p \end{aligned} \tag{4}$$

where the first expression is readily obtained by comparison of the first line of (1) and $A_{\ell p} = \frac{1}{2}(V_{\ell p} + Z_r I_p)$; similarly the second expression is deduced by comparison of the second line of (1) and $B_{\ell p} = \frac{1}{2}(V_{\ell p} - Z_r I_p)$.

The transient scattering equations relating the load voltage waves are obtained from (3), with the use of (4), *i.e.*,

$$\begin{aligned} b_{\ell 1} &= s_{11r} * a_{\ell 1} + s_{21r} * a_{\ell 2} \\ &\quad + \frac{1}{2}(s_{11r} - \delta(t)) * e_1 + \frac{1}{2} s_{21r} * e_2 \\ b_{\ell 2} &= s_{21r} * a_{\ell 1} + s_{11r} * a_{\ell 2} \\ &\quad + \frac{1}{2} s_{21r} * e_1 + \frac{1}{2}(s_{11r} - \delta(t)) * e_2. \end{aligned} \tag{5}$$

The set of transient equations for the wave variables $a_{\ell p}$ and $b_{\ell p}$ is completed by the equations describing the reflections from the two terminal circuits that load the line:

$$-y_r * (a_{\ell p} - b_{\ell p}) = g_p(a_{\ell p} + b_{\ell p}), \quad p = 1,\ 2 \tag{6}$$

where $y_r(t)$ is the transient expression of the reference admittance. The wave reflected from the load is caused by the "mismatch" between the reference admittance and the load characteristic g_p.

A relevant feature of our formulation is that the generator terms are included in the linear subset of the system equations, *i.e.* in the line scattering equations (5). In fact, the signals that enter and propagate along the line are decomposed into two contributions: one, $a_{\ell p}$, is due to the waves reflected by the loads, and the other, $\frac{1}{2} e_p$, depends on the excitation of the generators. The advantage of such decomposition results both in clarifying the physical mechanisms involved in the transient process, and in helping the explanation, carried out in the next section, of the role of the reference impedance Z_r in the solution procedure. The usual definition of the wave variables at the line ends would, however, include the generators in the nonlinear load equations and obscure the physical interpretation: the implications of this choice are discussed in Section V.A

For multiconductor lines, the unknown variables become the vectors $\mathbf{v_1}, \mathbf{v_2}, \mathbf{i_1}, \mathbf{i_2}$, that contain the voltages and currents at line ends 1 and 2 for each of the N conductors. The voltage waves

$$\begin{aligned} \mathbf{v_p} &= \mathbf{a_p} + \mathbf{b_p} \\ \mathbf{i_p} &= \mathbf{y}_r^{\square} * (\mathbf{a}_p - \mathbf{b}_p),\ p = 1, 2 \end{aligned} \tag{7}$$

are defined with respect to a reference impedance matrix, usually specified in the frequency domain, *i.e.* $\mathbf{Y}_r^{\square} = (\mathbf{Z}_r^{\square})^{-1}$. The transient scattering equations relate the voltage waves at the two line ends:

$$\begin{aligned} \mathbf{b}_1 &= \mathbf{s}_{11r}^{\square} * \mathbf{a}_1 + \mathbf{s}_{21r}^{\square} * \mathbf{a}_2 \\ \mathbf{b}_2 &= \mathbf{s}_{21r}^{\square} * \mathbf{a}_1 + \mathbf{s}_{11r}^{\square} * \mathbf{a}_2 \end{aligned} \tag{8}$$

where $\mathbf{s}_{21r}^{\square}$ and $\mathbf{s}_{11r}^{\square}$ are the $N \times N$ scattering matrices of the line, that is characterized by its impedance matrix $\mathbf{Z}_o^{\square}(\omega)$ and its mode propagation constants $\{K_i(\omega)\}$, $i = 1, \ldots, N$ [18]. Finally, the terminal loads are assumed to be multiport networks described by the nonlinear vector characteristics $-\mathbf{i_p} = \mathbf{g}_p(\mathbf{v}_{\ell p})$, $p = 1, 2$.

Although the multiconductor case is of paramount importance in the applications, the basic features of the problem are already contained in the scalar case and, for the sake of simplicity, we will refer to the latter wherever possible.

III. Effects of the Reference Impedance

As anticipated in the previous section, the choice of the reference impedance Z_r affects the actual form of various elements of the transient equations (5) and (6). The reference impedance need not be the same at the two line ends and, as a general rule, reference impedances similar to the line loads reduce their reflections and simplify the load equations at the expense of the complexity of the line characterization, *i.e.* of the impulse response functions s_{11r} and s_{21r}.

In order to illustrate this idea, we consider a simplified, linear form of the problem defined in Section II. We assume $e_1(t) = e_o\delta(t)$, $e_2(t) = 0$, $-i_1 = 1/Rv_{\ell 1}$, $-i_2 = 1/Rv_{\ell 2}$, (R being the value of the linear termination resistances), and the two extreme cases: (1) $Z_r = Z_o$, (2) $Z_r = R$.

Case (1): The line response is the simplest possible: $S_{11r} = 0$, $S_{21r} = H(\omega) = \exp\{-jK(\omega)\mathcal{L}\}$, which amount to a null reflection impulse response and to a delayed single-peak transmission impulse response $h(t)$. It is worthwhile to notice that $h(t) = 0$, for $t < \tau = \mathcal{L}\sqrt{LC}$, L and C being the per-unit-length inductance and capacitance of the line, respectively [14].

The load equations are given by the reflection coefficient of the resistance load R with respect to the reference impedance $Z_r = Z_o$, which is frequency dependent, and they take the

complicated expression

$$a_{\ell p} = \mathcal{F}^{-1}\left\{\frac{R - Z_o(\omega)}{R + Z_o(\omega)}\right\} * b_{\ell p},\ p = 1, 2. \tag{9}$$

The transients along the line are described by (5) that, in this case, assume a simpler form:

$$\begin{aligned} b_{\ell 1} &= h * a_{\ell 2} - \frac{1}{2} e_o \delta(t) \\ b_{\ell 2} &= h * a_{\ell 1} + \frac{1}{2} e_o h \end{aligned} \tag{10}$$

which we can interpret as a multiple reflection process of the input impulse between the two mismatched loads.

Case (2): The load equations are the simplest possible, since $Z_r = R$ force the reflected wave at the load to be zero, $a_{\ell p} = 0$. The complete solution solely depends on the $b_{\ell p}$ terms, *i.e.*

$$\begin{aligned} v_{\ell 1} &= b_{\ell 1} = \frac{1}{2} e_o (s_{11r} - \delta(t)) \\ v_{\ell 2} &= b_{\ell 2} = \frac{1}{2} e_o s_{21r} \end{aligned} \tag{11}$$

where the voltage waves result in sequences of echoes that are, in general, of complicated form. In other words, the transient is described with a fictitious matched scattering process such that the load information is completely contained in the line responses s_{pqr}.

These two cases suggest the following interpretation of the general problem (5), (6). When a reference impedance different from Z_o is adopted, the actual scattering process is replaced by an equivalent one where the load reflection is determined by the mismatch of the load with respect to Z_r and the scattering functions s_{pqr} account for the difference between Z_r and Z_o. Reference impedances that reduce the load reflections, *i.e.* such that the functions $|g_p(a_{\ell p} + b_{\ell p}) - y_r * (a_{\ell p} + b_{\ell p})|$ are small, result in a better matched scattering process, where part of the load effects is already included in the multiple echo scattering functions. Of course, this choice implies a simplification of the load equations at the expense of the line impulse response functions. In practice, the scope of reducing the load reflections can be achieved by appending the linear part of the loads to the line section, as suggested in [10], and/or equating Z_r to the impedance of the nonlinear load linearized around its working point. The analysis of the transient problem is then performed in two successive steps: the composite impulse responses are first evaluated via an inverse transformation of the transfer functions computed in the frequency domain, and the simplified scattering process is then solved in the time domain. Obviously, this technique is advantageous only for scattering functions with non critical inverse transforms. Finally, it should be remarked that the properties of the scattering process discussed in this section are inherent in the transient equations (5), (6), and the complexity of the computation is expected to depend on the behavior of the scattering parameters, irrespective of the algorithm used for their solution.

TABLE I
PARAMETER VALUES OF THE EXAMPLE

line length	$\mathcal{L} = 0.5$ m
voltage source	$e(t) = \begin{cases} v_o t & 0 < t < .5 \text{ ns} \\ 1 & .5 < t < 5.5 \text{ ns} \\ -v_o(t - t_o) & 5.5 < t < 6 \text{ ns} \\ 0 & \text{otherwise} \end{cases}$ $v_o = 2 \times 10^9$ V/s, $\quad t_o = 6$ ns
diode characteristic	$i_d = 10^{-8}(\exp(40 v_d) - 1)$ A
line L matrix	$L_{11} = L_{22} = 309$ nH/m $L_{12} = L_{21} = 21.7$ nH/m
line C matrix	$C_{11} = C_{22} = 144$ pF/m $C_{12} = C_{21} = -6.4$ pF/m
line R matrix	$R_{11} = R_{22} = 2.09 \times 10^{-4}\sqrt{\omega}\ \Omega$/m $R_{12} = R_{21} = 1.35 \times 10^{-5}\sqrt{\omega}\ \Omega$/m

IV. Reference Impedance for Lossy Lines

In order to decide whether a simple line characterization or simple load equations are preferable, the characteristics of the matched-line impulse response must be considered: line losses are the primary factors affecting the decision.

We limit the analysis to transmission lines in ideal dielectric media, for which two cases of particular relevance are distinguished. Appendix I is devoted to a discussion of the rationale for this classification. The first case refers to a high-loss line, whose impulse response $h(t)$ is mainly due to the wire DC resistance; this case is individuated by $R_{\mathrm{DC}}\mathcal{L} > 2Z_{\mathrm{LC}}$, where R_{DC} is the line DC resistance per unit length and Z_{LC} is the characteristic impedance of the line without losses ($Z_{\mathrm{LC}} = \lim_{\omega\to\infty} Z_o$). The second case, individuated by the complementary condition $R_{\mathrm{DC}}\mathcal{L} < 2Z_{\mathrm{LC}}$, denotes a low-loss line, whose response $h(t)$ is influenced by the high frequency skin losses. Examples of high-loss lines are the micrometric connections on integrated circuits, whereas all other types of interconnects usually satisfy the above low-loss condition (see Table I of [15] for typical numerical values of R_{DC} and $\mathcal{L}$).

For high-loss lines, the duration of the time response $h(t)$ is comparable or larger than the line propagation delay (see Appendix I) and, therefore, the impulse responses s_{pqr} are well behaved functions, readily obtainable from the corresponding functions in the frequency domain, via an inverse FFT. This means also that the load equations (6) can be effectively simplified by including all possible linear parts of the loads in the line characterization, and by numerically computing the impulse responses of the resulting two-port circuit (as already recommended in [10]). It is ought to remark that the normalization with respect to different impedence levels at the two line ends or the inclusion of linear parts of the loads in the line characterization breaks the symmetry relations $s_{11r} = s_{22r}$, $s_{21r} = s_{12r}$, and requires the evaluation of four impulse responses instead of two. The overall complexity of the solution procedure, however, is not affected, since the evaluation of the line response amounts to four convolutions in any case.

Low-loss lines, on the other hand, require special care for their characterization, since the high frequency losses produce a fast structure, with a duration w much smaller than τ, in

the early stages of the line response (see Appendix I). In this case, any choice of the reference impedance different from Z_o produces multiple-echo impulse responses that are made of short pulses (duration w), spaced by many times their duration. Impulse responses with these characteristics are unpractical for two reasons. Firstly, it is extremely difficult to obtain such responses via an inverse FFT, because the required Nyquist frequency is on the order of $1/w$ and their spectra must be described with a frequency resolution $1/\tau \ll 1/w$, thus requiring a large amount of data: this inversion problem arises already for impulse responses composed of simply two peaks spaced by τ. Secondly, the same large amount of data needed for a correct frequency approximation is required for the time representation of the impulse responses, and this lengthens the convolution computation of the transient solutions of (5) and (6). The optimum characterization of low-loss lines is therefore defined by $Z_r = Z_o$, leading to $s_{11r} = 0$, $s_{21r} = h(t)$.

However, this characterization implies also the computation of a second function, *i.e.* the transient admittance $y_o(t)$, that appears in the convolution of the load equations (6). Such function can be hardly obtained via the FFT, since $Y_o(\omega)$ does not vanishes for $\omega \to \infty$ and, y_o diverges for $t \to 0$, due to the skin effect (see Appendix II). The transient admittance, however, can be effectively computed through numerical inversion of its Laplace transform, by means of Padé approximation method [16], or Hosono algorithm [17][1]. In Appendix II it is also shown that, for transient signals shorter than a characteristic time t_y, the admittance y_o can be approximated by $y_o \approx Y_{\mathrm{LC}}\delta(t)$, with $Y_{\mathrm{LC}} = 1/Z_{\mathrm{LC}}$. The time scale t_y is inversely proportional to the factor assessing the line losses (*i.e.* $R_{\mathrm{DC}}\mathcal{L}/Z_{\mathrm{LC}}$), and for very low-loss lines (*i.e.* $R_{\mathrm{DC}}\mathcal{L} \ll Z_{\mathrm{LC}}$) it can be longer than the signal duration. Thus, for very low-loss lines, the convolution involving y_o in (6) can be avoided and the line can be completely specified by its impulse response $h(t)$, and the constant parameter Y_{LC} only. This line characterization is equivalently defined by $Z_r = Z_{\mathrm{LC}}$ and by approximating the responses s_{pqr} with those of the perfectly matched line ($s_{21r} \approx h$, $s_{11r} \approx 0$).

As a simple extension, in low-loss multiconductor transmission lines the optimum reference impedance matrix is $\mathbf{Z}_o^{\square}$, and $\mathbf{Z}_{\mathrm{LC}}^{\square} = \lim_{\omega\to\infty} \mathbf{Z}_o^{\square}(\omega)$ is recommended for very low losses and fast excitation signals. Diagonal reference impedance matrices (*i.e.* matching networks made of series impedances) are not appropriate, since they produce a mismatch sufficient to cause multiple-echo impulse responses, even for very low-loss lines and moderate coupling among the conductors (see the example in Section VI).

V. Comparison with Other Transient Equation Sets

In this section, we review other published methods for the transient analysis of nonlinearly loaded transmission lines, in order to compare the different formulations and their features, without considering the solution algorithms proposed, which are, in general, independent of the formulation. The structure of Fig. 1 (or its multiconductor extension), and the system scattering equations discussed in Section II are taken as the reference elements for the comparisons. A striking result of this section is that the reference impedance Z_r is the key parameter accounting for the differences among the formulations. The order in which the various methods are analyzed reflects the apparent differences with respect to our formulation.

[1] These algorithms are also well suited for the description of the line impulse response, in the case of low losses, since the FFT may be inefficient to reproduce both the early-time fast behavior and the late-time evolution of $h(t)$.

A. Scattering Parameter Method [4], [7], [9]

The transient equations proposed by Schutt-Aine and Mittra in [4], [7] and by Komuro in [9] are the same, and do not significantly differ from ours. In fact, the variables are the voltage waves at the line ends defined in (1), the line equations are the scattering equations (3), and the load equations are

$$-y_r * (a_p - b_p) = g_p(a_p + b_p - e_p), p = 1, 2, \qquad (12)$$

which differ from (5) and (6) only for the position of the generator terms.

From the computational point of view, the two sets of equations can be considered equivalent. In both cases, one proceeds by using the line equations (5) or (3) to eliminate the b variables from the load equations (6) or (12), respectively. This results in two nonlinear integral equations for the a unknowns, and the complexity of this problem, in term of number of convolution and nonlinear operations, is the same for the two formulations (5) and (6) or (3) and (12). With our formulation, however, the physical insight in the transient process is easier, because the contributions to terminal reflection terms of both the load reflection and generator act separated in (5) and (6), while they are lumped together in (12).

For the reference impedance used to define the voltage waves, Schutt-Aine and Mittra recommend $Z_r = Z_{\mathrm{LC}}$ for the single line problem [4], and $\mathbf{Z}_r^{\square} = \mathbf{Z}_{\mathrm{LC}}^{\square}$ for the multiconductor case [7], whereas Komuro [9] does not give any indications. The above form of the transient equations and the normalization suggested for the scattering parameters agree with our results of Sections II and IV, and constitute an effective method of analysis of very low-loss multiconductor lines.

B. Modified Scattering Parameter Method [5], [10]

In [5], [10], Gu et al. proposed a set of transient scattering equations with unknown voltages and currents. More precisely, in [10], the variables are the voltages and currents $v_{\ell p}$, i_p ($p = 1, 2$), defined in the load sections (Fig. 1), and the line equations are obtained by replacing in (5) the load voltage waves with their definitions in terms of voltages and currents, *i.e.*

$$\begin{aligned}(v_{\ell 1} - z_r * i_1) &= s_{11r} * (v_{\ell 1} + z_r * i_1) + s_{21r} * (v_{\ell 2} + z_r * i_2) \\ &\quad + (s_{11r} - \delta(t)) * e_1 + s_{21r} * e_2 \\ (v_{\ell 2} - z_r * i_2) &= s_{21r} * (v_{\ell 1} + z_r * i_1) + s_{11r} * (v_{\ell 2} + z_r * i_2) \\ &\quad + s_{21r} * e_1 + (s_{11r} - \delta(t)) * e_2. \end{aligned} \qquad (13)$$

Since the line impulse responses are still the scattering parameters s_{pqr}, the structure of the line equations remain similar to (5) and the method appears computationally equivalent to

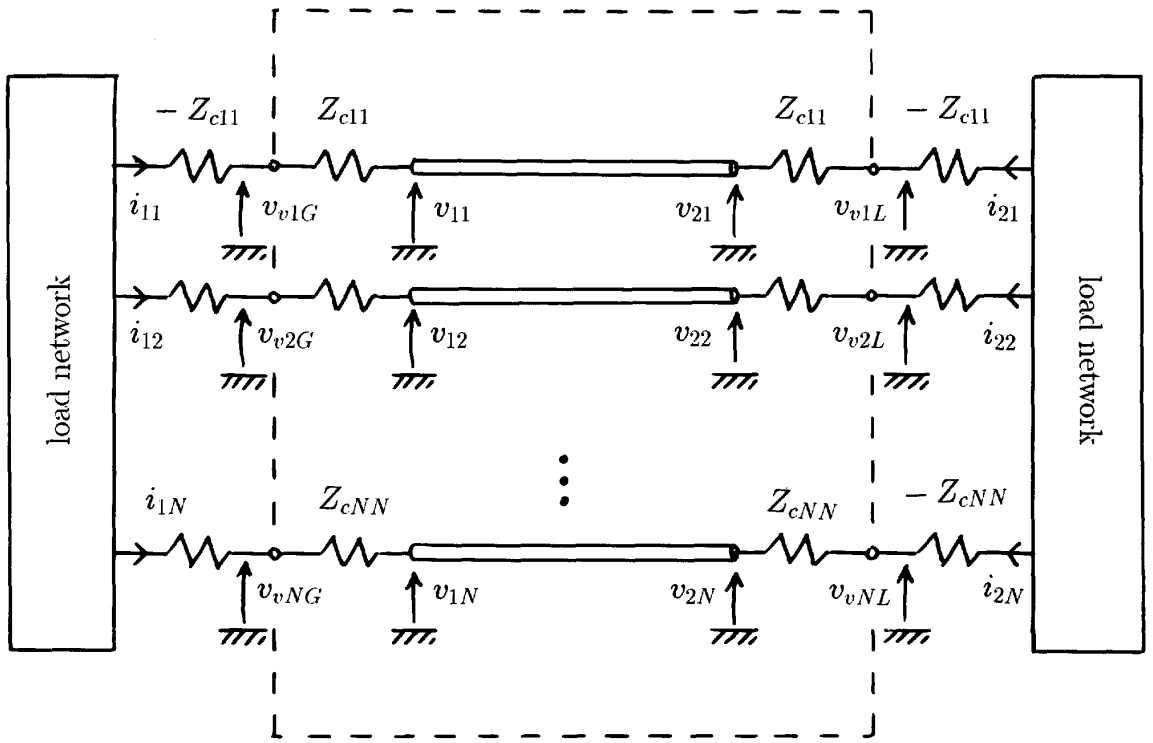

Fig. 2. Network representation suitable for the Y parameters method [3] and its modified version [8]. The dashed box defines the *augmented* line, and v_v's are the virtual voltages.

those using voltage waves. The equivalence can be verified with the elimination of i_1 and i_2 in (31) through the use of the load characteristics, $-i_p = g_p(v_{\ell p})$, $p = 1, 2$. For example, in the simple case $Z_r = Z_o$, the final equation for $v_{\ell 1}$ is

$$(v_{\ell 1} + z_o * g_1(v_{\ell 1})) = h*(v_{\ell 2} - z_o * g_2(v_{\ell 2})) - e_1 + h * e_2 \quad (14)$$

and must be compared with the final equation for $a_{\ell 1}$, obtained by eliminating $b_{\ell 1}$ of (5) in (6),

$$y_o * \left(a_{\ell 1} - \left(h * a_{\ell 2} - \frac{1}{2} e_1 + \frac{1}{2} h * e_2 \right) \right) = g_1 \left(a_{\ell 1} + \left(h * a_{\ell 2} - \frac{1}{2} e_1 + \frac{1}{2} h * e_2 \right) \right). \quad (15)$$

The complexity of the two equations is equivalent, although the variables are not the same. On the other hand, the physical interpretation is helped when voltage waves are used.

With respect to the choice of the reference impedance, Gu et al. use $\mathbf{Z}_r^{\square} = \text{diag}\{\mathbf{Z}_{\text{LC}}^{\square}\}$ in [5], which is devoted to purely dispersive lines, while in [10] they use $\mathbf{Z}_r^{\square} = \text{diag}\{Z_{oi}\}$, where Z_{oi} is the characteristic impedance of the line connected to the i-th load. As discussed in Section IV, for low-loss lines, this choice can lead to multiple-echo impulse responses even for weakly coupled conductors. Finally, the inclusion of all possible linear load component in the line characterization is suggested in [10].

C. Admittance Y Parameter Method [3]

The work of Djordjevic et al. [3] is a pioneering one on the subject of nonlinearly loaded transmission lines. The unknowns of their transient equations are the voltages and currents at the line ends, and the line response is described in terms of the admittance Y parameters.

The use of the Y parameters was subsequently criticized, as they were believed to yield impulse responses with infinite many echoes. The criticism, however, is not appropriate, since it does not take into account the particular definition of the Y parameters, that are defined in [3] with respect to auxiliary variables with a special physical meaning, called *virtual voltages* and indicated in Fig. 2 with the symbols v_{viG}, v_{viL}, $(i = 1, \ldots, N)$, where the G and L subscripts stand for the generator and load side of the line, respectively, and N is the number of conductors. In fact, the virtual voltages coincide, apart from a factor two, with the voltage waves reflected by the loads and defined with respect to the reference impedances $Z_{ri} = Z_{cii}$. This is readily shown in the scalar case (*i.e.* $i = 1$ only), for which the frequency domain virtual voltages are

$$V_{vG} = V_1 + Z_c I_1 = [V_1 + Z_r I_1]_{Z_r = Z_c} = 2[A_1]_{Z_r = Z_c}$$
$$V_{vL} = V_2 + Z_c I_2 = [V_2 + Z_r I_2]_{Z_r = Z_c} = 2[A_2]_{Z_r = Z_c} \quad (16)$$

As a consequence, the Y parameters are simple linear combinations of the line scattering parameters defined for $Z_r = Z_c$. Again, this result is readily shown for the scalar case, in the frequency domain. The Y parameters are defined with

reference to the network in the dashed box (*the augmented line*) of Fig. 2, *i.e.*

$$I_1 = Y_{11}V_{vG} + Y_{21}V_{vL} = Y_{11}(V_1 + Z_rI_1) + Y_{21}(V_2 + Z_rI_2)$$
$$I_2 = Y_{21}V_{vG} + Y_{11}V_{vL} = Y_{21}(V_1 + Z_rI_1) + Y_{11}(V_2 + Z_rI_2) \quad (17)$$

where the simmetry of the line is exploited, and (16) are used. The scattering equations (3), written in the frequency domain and in terms of voltages and currents with the help of (1), become

$$(V_1 - Z_rI_1) = S_{11r}(V_1 + Z_rI_1) + S_{21r}(V_2 + Z_rI_2)$$
$$(V_2 - Z_rI_2) = S_{21r}(V_1 + Z_rI_1) + S_{11r}(V_2 + Z_rI_2) \quad (18)$$

and can be cast, after a little manipulation (*i.e.* addition of the terms $-(V_1 + Z_rI_1)$ and $-(V_2 + Z_rI_2)$ to the first and second equation above, respectively, and division by $-2Z_r$), in a form comparable with (17). The comparison shows the direct relationship between Y and S parameters:

$$Y_{11} = \frac{S_{11r} - 1}{-2Z_r}, \qquad Y_{21} = \frac{S_{21r}}{-2Z_r}. \quad (19)$$

For a multiconductor line, the same results hold, provided that $\mathbf{Z}_r^{\square} = \text{diag}\{Z_{cii}\}$. Since in [3] the impedances Z_{cii} represent the diagonal elements of the matrix $\mathbf{Z}_{\text{LC}}^{\square}$, the reference impedance of this method is $\mathbf{Z}_r^{\square} = \text{diag}\{\mathbf{Z}_{\text{LC}}^{\square}\}$, that can however produce multiple-echo impulse responses.

Finally, a further criticism to the method of [3] concerns the negative impedance $-Z_{cii}$ needed to define the augmented line. Numerical instabilities in the solution of low-loss lines have been attributed to the presence of such impedances [5], but they do not seem to be the cause, since the line equations hold independently of these impedances. We rather believe that numerical instabilities may be due to a line characterization that implies a multiple-echo impulse response. In fact, as discussed in Section III, a choice of Z_r different from the load value causes the actual solution to arise from multiple back-and-forth reflections of the line impulse response, and in such case instabilities may develop.

D. Modified Y Parameter Method [8]

Winkelstein et al. propose in [8] a modified version of the previous method. They replace the Y parameters with the scattering ones in the line characterization, in an attempt to obtain better-behaved impulse response functions. Of course, it is illusory that such change can make the difference, since the Y and S parameters are strictly related (see (19)), and the reference impedance is the only element that controls the behavior of the impulse responses.

The line equations of [8], written for the scalar case and in the frequency domain (our symbols Z_c, V_{vG}, V_{vL} stand for Z_m, V_1', V_2' of [8]), are

$$V_1 = G_{11}V_{vG} + G_{21}V_{vL}$$
$$V_2 = G_{21}V_{vG} + G_{11}V_{vL} \quad (20)$$

that are a non conventional description of the linear elements contained in the dashed box of Fig. 2 and the G_{pq}'s represent the transfer functions.

The relationship between the transfer functions $G_{pq}(\omega)$ and the scattering parameters defined for $Z_r = Z_c$ can be obtained with the same steps of Section V.C (*i.e.* addition of $(V_1+Z_rI_1)$ and $(V_2 + Z_rI_2)$ to the first and the second equation (18), respectively), and become

$$G_{11} = \frac{S_{11r} + 1}{2}, \qquad G_{21} = \frac{S_{21r}}{2}. \quad (21)$$

A comparison of (21) and (19) indicates that this formulation is essentially equivalent to [3]. Therefore, despite the claims of [8], the introduction of the scattering parameters (whose reference impedance value Z_r is not specified in [8]) yields no advantages with respect to [3].

E. Method of Characteristics [2, 6]

In [2, 6], the generalized method of characteristics is exploited for the line characterization, and a simple equivalent of the line is proposed. This approach was then followed by many other authors (*e.g.*, see [12] for a remarkable generalization that extends the method to hybrid-mode structures) and its formulation is now one of the most established in the study of transmission lines.

The approach of the method of characteristics is equivalent to a scattering parameter characterization defined for $Z_r = Z_o$. In fact, with reference to the notation of [6], the equivalent circuit for the line is defined by

$$(V_1 - Z_{01}I_1) = e^{\theta_1}(V_2 + Z_{02}I_2)$$
$$(V_2 - Z_{02}I_2) = e^{\theta_2}(V_1 + Z_{01}I_1) \quad (22)$$

where Z_{01}, Z_{02} are the line characteristic impedances at the ends 1 and 2, respectively (the method can account for nonuniform asymmetric lines), and the exponential functions are the transmission transfer functions of the matched line.

For a uniform line (*i.e.* $Z_{01} = Z_{02} = Z_o$, $\theta_1 = \theta_2 = -jK(\omega)\mathcal{L}$), the above equations coincide with the scattering equations (see 18), provided that the reference impedance is $Z_r = Z_o$, so that $S_{11r} = 0$ and $S_{21r} = H(\omega) = \exp\{-jK(\omega)\mathcal{L}\}$.

In conclusion, this approach can effectively handle low loss lines, since it is based on a characterization that uses $Z_r = Z_o$ (see Section IV). Also, the simple equivalent circuit introduced by this method turns out to be useful for CAD implementations.

F. Chain Parameter Matrix Method [11]

Recently, Mao and Li [11] published an analysis of nonuniform transmission lines, possibly terminated on nonlinear loads, by means of the chain parameter matrix,

$$\begin{pmatrix} V_1 \\ I_1 \end{pmatrix} = \begin{pmatrix} \mathcal{A} & \mathcal{B} \\ \mathcal{C} & \mathcal{D} \end{pmatrix} \begin{pmatrix} V_2 \\ -I_2 \end{pmatrix} \quad (23)$$

where

$$\mathcal{A} = \frac{1}{2}(\exp\{+jK\mathcal{L}\} + \exp\{-jK\mathcal{L}\})$$
$$\mathcal{B} = \frac{Z_o}{2}(\exp\{+jK\mathcal{L}\} - \exp\{-jK\mathcal{L}\})$$

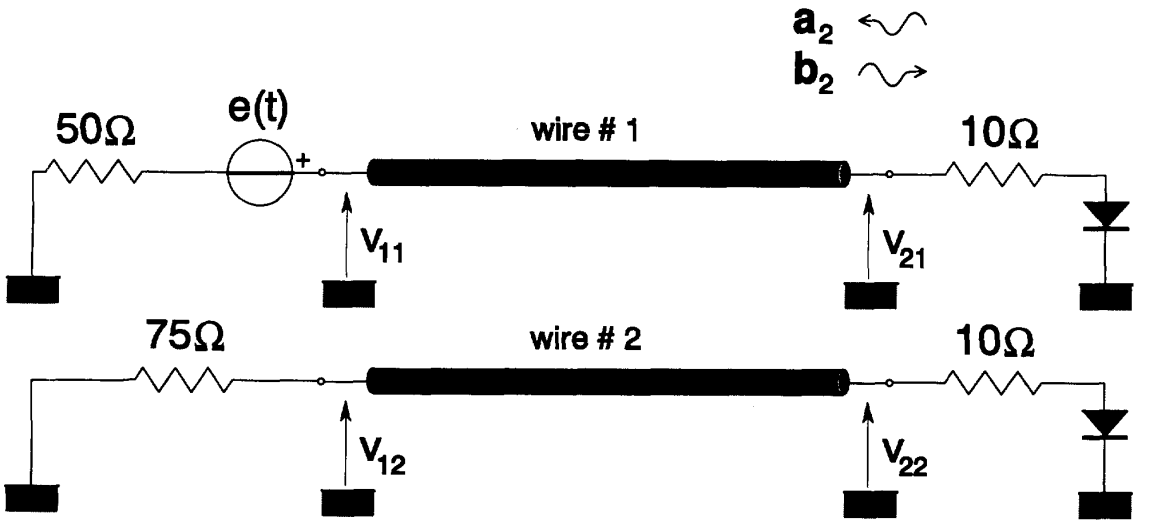

Fig. 3. Network for the numerical example of Section VI. The time function of the source, the diode characteristic and the line parameters are listed in Table I.

$$\mathcal{C} = \frac{1}{2Z_o}(\exp\{+jK\mathcal{L}\} - \exp\{-jK\mathcal{L}\})$$
$$\mathcal{D} = \frac{1}{2}(\exp\{+jK\mathcal{L}\} + \exp\{-jK\mathcal{L}\}).$$

These equations connect directly the voltages and currents at the two ends of the line, and are suitable for the response computation of cascaded lines. Also, (23) yields particularly simple transient equations, in the time domain.

Although the transfer functions $\mathcal{A}$, $\mathcal{B}$, $\mathcal{C}$, and $\mathcal{D}$ are related to the line scattering parameters (it is readily shown that (23) is obtained from (18), for $Z_r = Z_o$, so that $S_{11r} = 0$ and $S_{21r} = H(\omega) = \exp\{-jK(\omega)\mathcal{L}\}$), they have different properties.

In order to focus on the physical meaning of the impulse responses obtainable in this case, let us consider the voltage behavior at the near end of an ideal transmission line (*i.e.* one with $K(\omega) = \omega/v$), whose far end is left open. The result

$$[v_1(t)]_{i_2=0} = \frac{1}{2}\left(\delta\left(t + \frac{\mathcal{L}}{v}\right) + \delta\left(t - \frac{\mathcal{L}}{v}\right)\right) * v_2(t) \quad (24)$$

is the time domain expression of the first equation of (23), and depends on both past and future values of $v_2(t)$. Such non-causality of the impulse responses complicates the use of a time stepping algorithm for the solution of the transient equations.

This problem worsens when real dispersive or lossy lines are considered. In this case, $\alpha(t) = \frac{1}{2}\mathcal{F}^{-1}\{\exp(+jK\mathcal{L}) + \exp(-jK\mathcal{L})\}$ does not exist, since $\exp\{jK(\omega)\mathcal{L}\}$ is exponentially growing for $|\omega| \to \infty$. In [11], this difficulty does not appear, because the exponentials of the transfer functions are approximated with truncated power series, resulting in analytical approximations of the impulse response functions. These approximations certainly hold for input signals having a bandwidth small with respect to the bandwidth of $H(\omega)$, but this aspect is not discussed quantitatively in [11]. A final remark is in order here, that a power series approximation of the propagation exponentials deletes the propagation delay effect and gives always rise to a transmission impulse response with non causal parts (*e.g.*, this is clearly seen in the plot of the variable V4, in Fig. 6 of [11]).

The line description with the chain parameter matrix, therefore, does not seem to have significant advantages, when compared with the conventional scattering parameter description.

VI. Numerical Example

The scope of this section is to illustrate with an example the concepts that are extensively discussed in Section IV, *i.e.* the influence of the line characterization on the solution method and on the accuracy of the results. In particular, we compare the features of the solutions obtained with different normalizations (*i.e.* $\mathbf{Z}_r^{\square} = \mathrm{diag}\{\mathbf{Z}_{\mathrm{LC}}^{\square}\}$, $\mathbf{Z}_r^{\square} = \mathbf{Z}_o^{\square}$, and $\mathbf{Z}_r^{\square} = \mathbf{Z}_{\mathrm{LC}}^{\square}$), for a low-loss weakly coupled multiconductor line.

A. Network Characteristics

The network of the example is shown in Fig. 3 and contains a symmetric line made of two conductors and a ground plane, with linear loads at one end, and nonlinear elements at the other end. We adopt the same example of the fundamental paper by Djordjevic et al. [3], in order to compare the results. The numerical values of the source, load and line parameters are summarized in Table I. The line conductance matrix given in [3] is neglected, as it affects only the very high frequency part of the line characterization.

For convenience, we adopt a modal representation to describe the signal propagation along the line. A short summary of the properties of the *even* and *odd* modes of a three-conductor line is given in Appendix IV. The advantage of the modal description is that it allows a direct generalization of the treatment of the scalar problem. The transfer function H and the characteristic impedance Z_o of the scalar case are

TABLE II
MODAL PARAMETERS

	even mode	odd mode
R_o	$R_{oe} = 2.23 \times 10^{-4}\ \Omega\sqrt{\text{s/rad}}$	$R_{oo} = 1.95 \times 10^{-4}\ \Omega\sqrt{\text{s/rad}}$
w	$w_e \approx 1.6$ ps	$w_o \approx 1.6$ ps
τ	$\tau_e = 3.373$ ns	$\tau_o = 3.287$ ns
$\mathbf{Z}^{\square}_{LCm} = diag\{Z_{LCe}, Z_{LCo}\}$	$Z_{LCe} \approx 49\ \Omega$	$Z_{LCo} \approx 43.7\ \Omega$

TABLE III
LINE CHARACTERIZATION PARAMETERS

	in Sec. 6	in [3]
reference impedance [Ω]		$\mathbf{Z}^{\square}_r = diag\{\mathbf{Z}^{\square}_{LC}\} \approx \begin{pmatrix} 46.4 & 0 \\ 0 & 46.4 \end{pmatrix}$
modal reference impedance [Ω]	$\mathbf{Z}^{\square}_{rm} = \mathbf{Z}^{\square}_{om} = \begin{pmatrix} 49 & 0 \\ 0 & 44 \end{pmatrix}$	
sampling pitch	variable	20 ps
number of samples in s_{pqr}	13 over 250 ps	512
number of samples in y_r	5 over 10 ns	

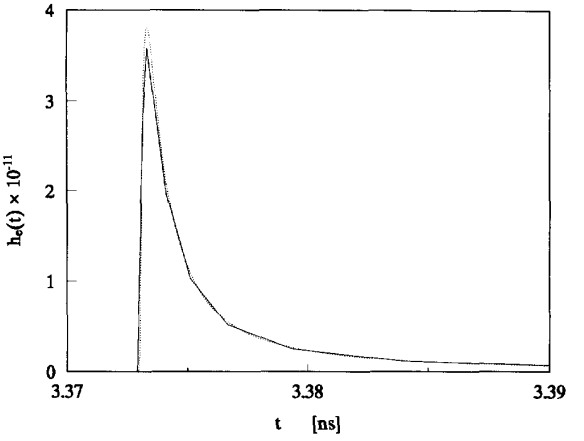

Fig. 4. Transmission impulse response for the even mode of the line in Fig. 3 (dotted line) and its piecewise linear representation adopted by the numerical solution (solid line). The approximation curve is scaled so that the correct pulse area is maintained. Please notice that the time axis begins at $t = 3.37$ ns, due to the mode delay.

simply replaced by the transfer functions H_e, H_o and the characteristic impedances Z_{oe}, Z_{oo} for the even and the odd mode. The modal parameters computed from the data of Table I are summarized in Table II.

Although the inequalities of Appendix I cannot be applied directly to this example, because the DC resistance is not known, the transfer functions H_e and H_o are of low-loss type, since they are mainly determined by the skin effect (see Appendix I and data of Table II). The line impulse responses h_e, h_o are then computed analytically as described in Appendix I and, consistently, their durations appear much shorter than the mode delays (see Table II). The impulse response $h_e(t)$ is shown by the dotted line of Fig. 4: its peak is located around $t = \tau_e + 0.5$ ps and its fast part extinguishes within a few ps. The odd-mode response $h_o(t)$ is barely distinguishable from h_e, and is not shown. For the numerical solution, the transient scattering parameters h_e, h_o are represented with piecewise linear functions defined on nonuniformly spaced time samples, as shown in Fig. 4. The location and the number of samples are selected to be compatible with a sufficient reproduction of both the fast initial part and the long tail of the functions. The cut-off time of the h_e, h_o tails are selected so that the pulse areas are approximately 1, as it is required by $H(0) = 1$. The same considerations apply for the transient admittances y_{oe}, y_{oo}, which however are represented analytically for small values of t, where they are singular. The parameters of the line characterization used for the solution are reported in Table 3, where data of [3] are also given for comparison.

A final remark concerns the effects of the normalization adopted by [3]. Their choice of the reference impedance leads to the following diagonal modal scattering matrices:

$$\mathbf{S}^{\square}_{11rm} = \text{diag}\{S_R(Z_{re}, Z_{oe}, H_e), S_R(Z_{ro}, Z_{oo}, H_o)\}$$
$$\mathbf{S}^{\square}_{21rm} = \text{diag}\{S_T(Z_{re}, Z_{oe}, H_e), S_T(Z_{ro}, Z_{oo}, H_o)\},$$

with $Z_{re} = Z_{ro} = 46.4\ \Omega$ and S_T, S_R defined in Appendix III. The time evolutions of such scattering parameters are affected by multiple reflections, while those of our proposed solution (for which $\mathbf{S}^{\square}_{11rm} = 0$ and $\mathbf{S}^{\square}_{21rm} = \text{diag}\{H_e, H_o\}$) show the regular behavior of Fig. 4.

B. Comparison of Results

The voltage waveforms obtained with the above parameters in the time interval $0 \le t \le 10$ ns are shown in Figs. 5 and 6, for both ends of wire 1 and 2, respectively. The solid curves refer to the results obtained for the normalization $\mathbf{Z}^{\square}_r = \mathbf{Z}^{\square}_o$, while the dashed lines are for $\mathbf{Y}^{\square}_o \approx \text{diag}\{Y_{\text{LCe}}, Y_{\text{LCo}}\}$. A small difference between the two solutions arises for the long pulses, while the shape of short pulses is unaffected by the approximation of the characteristic admittance. This is justifiable, since the parameter that measures the time scale on which the error build up (see Appendix II for a precise definition) is $t_y \approx 3.5$ ns, comparable with the duration of the excitation signal $e(t)$. This result confirms that very low-loss lines can be effectively described with a reflectionless characterization and a frequency independent reference impedance $\mathbf{Z}^{\square}_r = \mathbf{Z}^{\square}_{\text{LC}}$.

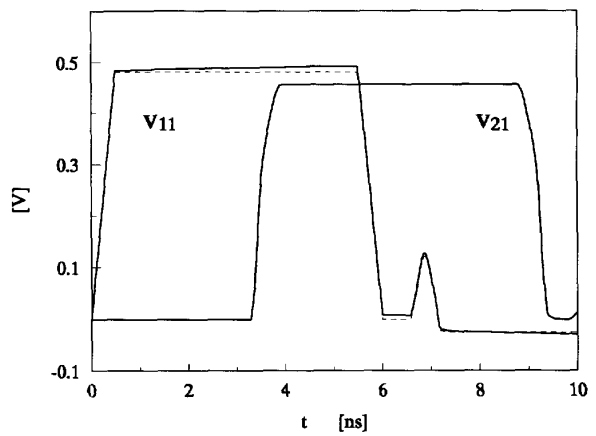

Fig. 5. Computed time domain voltage waveforms at the near end (v_{11}) and far end (v_{12}) of wire 1 in Fig. 3. The solid curves refer to the results obtained for the normalization $\mathbf{Z}_r^{\square} = \mathbf{Z}_o^{\square}$, while the dashed lines are for: $\mathbf{Y}_o^{\square} \approx \text{diag}\{Y_{LCe}, Y_{\text{LCo}}\}$.

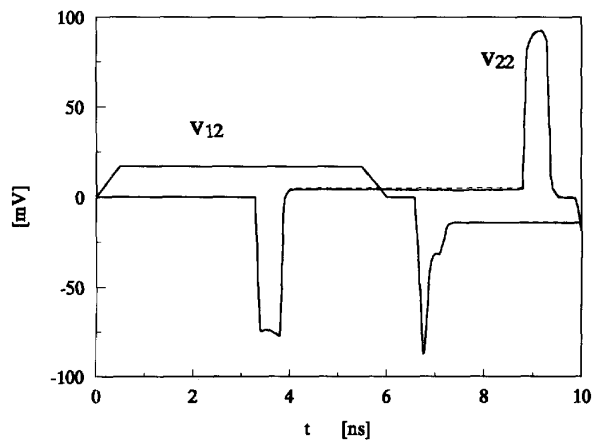

Fig. 6. Computed time domain voltage waveforms at the near end (v_{12}) and far end (v_{22}) of wire 2 in Fig. 3. The solid curves refer to the results obtained for the normalization $\mathbf{Z}_r^{\square} = \mathbf{Z}_o^{\square}$, while the dashed lines are for $\mathbf{Y}_o^{\square} \approx \text{diag}\{Y_{\text{LCe}}, Y_{\text{LCo}}\}$.

A comparison of the results of Figs. 5 and 6 with Fig. 5 of [3] indicates that the two solutions agree in their steady state levels, while there are differences in the shape and in the duration of the transient parts caused by the generator ramps. The differences are larger for the non-driven line, and this is almost certainly due to the insufficient precision with which the line impulse responses are represented in [3].

This lack of precision typically comes from the difficulties of the numerical evaluation and of the representation of multiple-echo impulse responses for low-loss lines, as discussed in Section IV. In fact, the reference impedance $\mathbf{Z}_r^{\square} = \text{diag}\{\mathbf{Z}_{\text{LC}}^{\square}\}$ adopted by [3] produces impulse responses with multiple echoes, that were numerically approximated with 512 samples spaced by 20 ps. We believe that this choice was forced by the consideration that convolutions with a larger number of points can considerably slow down the computer solution of the problem. However, this choice has two weaknesses: (1) the total duration of the impulse response is 10 ns that corresponds to almost three times the line delay, thus including only the transmitted pulse and its first reflected echo; (2) the time step of 20 ps is clearly insufficient to accurately represent the shape of the impulse response shown in Fig. 4.

In the network under analysis, the only memory effect comes from the visible duration of the impulse responses h_e, h_o (approximately 20 ps, see Fig. 4) and from the difference of the mode delays along the line (nearly 80 ps). Therefore, the allowed duration of the v_{21} and v_{22} transients due to the first arrival of the generator rising ramp is 0.6 ns, as it is in our solution. The anomalous duration of the transients in [3] (approximately 0.9 ns) are caused by contributions from non-causal tails of their impulse responses. Such noncausality, however, is evidenced by the non zero values of v_{21} at times shorter than the line delay.

The time plots of the even and odd components of the voltage wave vectors $\mathbf{b}_{2m}$ (impinging on load 2) and $\mathbf{a}_{2m}$ (reflected from load 2) shown in Fig. 7 are particularly useful because allow us to gain a physical insight into the effects that the nonlinearities produce on transients. At the transient start, the voltages at the far-end terminals are low and the apparent resistance of the diodes are much greater than Z_{LCe} and Z_{LCo}. However, since the two conductors are weakly coupled, the evolution is dominated by the characteristic of the load on the driven wire. Thus, for the initial part of the transient, the reflection coefficients in the far-end section are almost unity, *i.e.* $a_{2e} \approx b_{2e}$ and $a_{2o} \approx b_{2o}$, and the terminal voltages become

$$v_{21} = \frac{(a_{2e} + b_{2e}) + (a_{2o} + b_{2o})}{\sqrt{2}} \approx \sqrt{2}(b_{2e} + b_{2o})$$
$$v_{22} = \frac{(a_{2e} + b_{2e}) - (a_{2o} + b_{2o})}{\sqrt{2}} \approx \sqrt{2}(b_{2e} - b_{2o}). \quad (25)$$

These expressions constitute a useful mean to explain the numerical results shown in Figs. 5 and 6. For example, as the voltage v_{21} grows, the apparent resistance of the diode on wire 1 decreases, and so does the load reflection coefficient. This, in turn, reduces the voltage growth and stabilizes v_{21} to the value for which the load on wire 1 nearly matches the characteristic impedance of the wire. On the other wire, the evolution of v_{22} is controlled by the difference between the even and odd component of the impinging voltage wave vector. The final state (for $t > 3.8$ ns) depends only on the final values of the impinging voltage waves, which are controlled by the transmission impulse response areas.

The sensitivity of the solution of the non-driven wire to the impulse response accuracy grows when the difference between the mode delays reduces. In fact, if the two mode delays were equal, the starting slope of the v_{22} transient would be decided by the difference between the synchronous peaks of the functions h_e and h_o (see the second of (25)), and this is highly dependent on the precision of the calculations. Thus, the use of poorly represented impulse responses for low-loss symmetric multiconductor lines in homogeneous dielectric media, for which the mode speeds are equal [18], can lead to large errors on the nondriven wires.

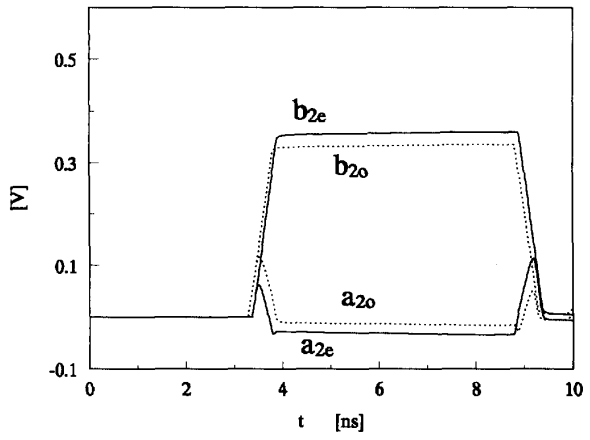

Fig. 7. Time domain behavior of the even (solid line) and odd components (dotted line) of the incident ($\mathbf{b}_{2m}$) and reflected ($\mathbf{a}_{2m}$) voltage wave vectors at the far end terminal of the line of Fig. 3.

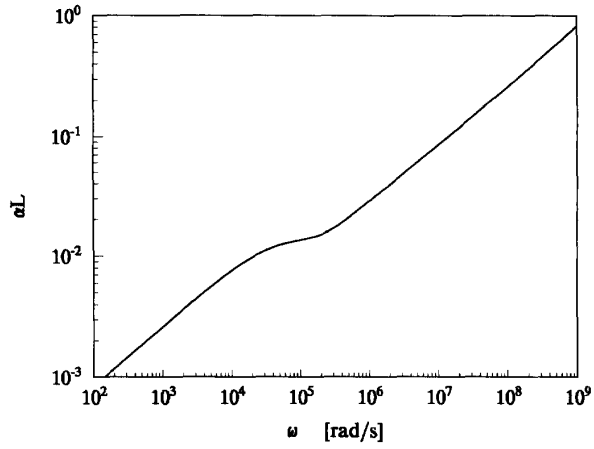

Fig. 8. Frequency behavior of the loss factor $\alpha\mathcal{L} = -\Im m\{K(\omega)\}\mathcal{L}$ for a RG-213/U coaxial cable with $\mathcal{L} = 92$ m.

The discussion of our example leads to the conclusion that the accurate representation of the impulse responses of low-loss lines affected by skin effect is difficult. The choice of $\mathbf{Z}_r^{\square} = \mathbf{Z}_o^{\square}$, or $\mathbf{Z}_r^{\square} = \mathbf{Z}_{\mathrm{LC}}^{\square}$ for very low-loss lines, and the analytic evaluation of the impulse responses offer numerical efficiency and improved accuracy not only for strongly-coupled multiconductor lines (which is trivial), but also for weakly-coupled multiconductor structures. Besides, in symmetric and homogeneous multiconductor lines, for which all modes have the same speed, the use of multiple-echo impulse responses is critical and is expected to produce large errors in the electrical quantities of the nondriven wires.

VII. Conclusion

In this paper, the influence of the reference impedance parameter on the structure of the transient equations that predict the signal evolution in nonlinearly loaded transmission lines is discussed.

The analysis is based on the new set of transient equations (5) and (6), that allow a deeper physical interpretation of the nonlinear process in the presence of distributed circuits. We show that the line classification according to the losses is relevant for the optimal choice of the line characterization, which in turn affects the solution algorithm. A precise definition of high- and low-loss lines and the implications on the corresponding transfer functions are given in Appendix I. The inclusion of linear parts of the loads in the line subcircuit, with the aim at simplifying the scattering process [10], is found to be advantageous for high-loss lines and potentially harmful to low-loss ones. The latter are better described with $\mathbf{Z}_r^{\square} = \mathbf{Z}_o^{\square}$, or with $\mathbf{Z}_r^{\square} = \mathbf{Z}_{\mathrm{LC}}^{\square}$ for very low losses and fast driving signals, thereby avoiding multiple echoes in the line impulse responses.

A comparative analysis of the main mixed methods published in the literature shows that all, except the one based on the chain parameter matrix [11], refer to a scattering parameter formulation. However, the fundamental role of the reference impedance is often overlooked. As far as the line is characterized with the scattering parameters, there are no appreciable computational differences in using voltages and currents or voltage waves as equation variables, but the latter are preferred, since they have a higher physical significance and help to better understand the process. The chain parameter matrix method is apparently simpler, but, owing to the non-causality of its impulse responses, is found to have a computational complexity comparable with the scattering parameter method. Also, an inappropriate criticism to the Y parameter method [3] is corrected by proving the equivalence of Y and S parameters.

The numerical example of Section VI is used to validate our findings of Sections III and IV and to check the performance of our approach in comparison with [3], where problems are expected to arise due the use of multiple-echo impulse responses. The results demonstrate that the normalizations suggested for low-loss lines, *i.e.* $\mathbf{Z}_r^{\square} = \mathbf{Z}_o^{\square}$ and $\mathbf{Z}_r^{\square} = \mathbf{Z}_{\mathrm{LC}}^{\square}$, are largely preferable for the computational efficiency and precision, even for weakly coupled transmission lines. Also, the example makes it evident that, for symmetric lines with homogeneous dielectric having the same speed for all modes, the solutions of non-driven wires are sensitive to the line description, and our formulation is more robust with respect to those describing the line with multiple-echo impulse responses.

Appendix I

The propagation constant of a transmission line with metal losses and ideal dielectric is

$$K(\omega) = \sqrt{-(R(\omega) + j\omega L)j\omega C} = \frac{\omega}{v}\sqrt{1 - j\frac{R(\omega)v}{\omega Z_{\mathrm{LC}}}} \quad (26)$$

where $R(\omega)$ is the line resistance per unit length, and $v = 1/\sqrt{LC}$. As an example of the frequency behavior of (26), Fig. 8 shows the attenuation $\alpha\mathcal{L} = -\Im m\{K(\omega)\}\mathcal{L}$ of the transfer function $H(\omega) = \exp\{-jK(\omega)\mathcal{L}\}$, for a RG-213/U coaxial cable.

In the low-frequency straight part of the $\log(\alpha)$-curve, the function $R(\omega)$ is determined by the ohmic DC losses, i.e., $R(\omega) \approx R_{\mathrm{DC}}$, where R_{DC} is the line DC resistance per unit

length, and the propagation constant is approximated by

$$K(\omega) \approx K_\Omega = (1-j)\sqrt{\frac{R_{DC}}{2Z_{LC}v}}\sqrt{\omega}. \tag{27}$$

In the high frequency straight part of the α curve, skin losses are dominant, *i.e.* $R(\omega) \approx (1+j)R_o\sqrt{\omega}$, where $R_o = \sqrt{k_g R_{DC}}$ is the skin parameter (the value of the coefficient k_g depends on the transverse geometry of the conductor [19]). For $\omega > \omega_s$ (with $\sqrt{\omega_s}R_o = R_{DC}$), the propagation constant is approximated by

$$K(\omega) \approx K_s = \frac{\omega}{v} + (1-j)\frac{R_o}{2Z_{LC}}\sqrt{\omega}. \tag{28}$$

The level of the plateau region in the $\log(\alpha)$-curve is $R_{DC}\mathcal{L}/2Z_{LC}$ and its value decides the bandwidth of $H(\omega)$. If $R_{DC}\mathcal{L}/2Z_{LC} > 1$ the bandwidth of $H(\omega)$ is limited to the low frequency part of $K(\omega)$ and the line is not influenced by skin losses (high-loss line), whereas if $R_{DC}\mathcal{L}/2Z_{LC} < 1$ the part of $K(\omega)$ dominated by skin losses contributes to $H(\omega)$ (low-loss line).

For high-loss lines the width of the impulse response w can be estimated as $w \approx 1/\omega_m$, where $-\Im m\{K_\Omega(\omega_m)\}\mathcal{L} = 1/3$, *i.e.* $w \approx 9\frac{R_{DC}\mathcal{L}}{2Z_{LC}}\tau$, and is therefore comparable or larger than τ. In low-loss lines the high-frequency approximation of $H(\omega)$ is $\exp\{-jK_s(\omega)\mathcal{L}\}$, which results in a short time part of $h(t)$ given by [18]

$$h_s(t) \approx \frac{1}{\eta}\frac{1}{\sqrt{\pi x^3}}\exp\left\{-\frac{1}{x}\right\} \tag{29}$$

$$x = \left(t - \frac{\mathcal{L}}{v}\right)/\eta, \qquad \eta = \frac{1}{8}\left(\frac{R_o\mathcal{L}}{Z_{LC}}\right)^2$$

which is a fast pulse of time duration $w = 2\eta = \frac{R_{DC}\mathcal{L}}{2Z_{LC}}\frac{k_g v}{2Z_{LC}}\tau \ll \tau$ (the factor k_g varies in the range $[10^{-8}, 5\times 10^{-8}]$ Ω/m s). Besides, for very low-loss lines, *e.g.* $R_{DC}\mathcal{L} < 0.1Z_{LC}$, the low frequency part of $K(\omega)$ is a negligible portion of the total bandwidth of $H(\omega)$ and $h(t)$ can be globally approximated with $h_s(t)$. We wish to point out that, in the very low-loss case, the numerical inverse transformation can hardly improve this approximation because the differences between $K(\omega)$ and $K_s(\omega)$ are confined in the range $\omega < \omega_s$ and $\omega_s \ll \omega_{max}$, ω_{max} being the angular frequency where $H(\omega)$ vanishes (*e.g.*, if $-\Im m\{K_s(\omega_{max})\}\mathcal{L} = \sqrt{10}$, $\omega_{max}/\omega_s = 10(2Z_{LC}/R_{DC}\mathcal{L})^2$).

APPENDIX II

The characteristic impedance of a line with pure metal losses is

$$Z_o = Z_{LC}K(\omega)\frac{v}{\omega} = Z_{LC}\sqrt{1 + \frac{R(\omega)v}{j\omega Z_{LC}}}. \tag{30}$$

The corresponding characteristic admittance is

$$Y_o(\omega) = 1/Z_o(\omega) = Y_{LC}/\sqrt{1 + \frac{R(\omega)v}{j\omega Z_{LC}}}, \quad Y_{LC} = 1/Z_{LC} \tag{31}$$

and

$$Y_o(\omega) \to \begin{cases} 0, & \text{for } \omega \to 0, \\ Y_{LC}\left(1 - \frac{R_o v}{\sqrt{2}Z_{LC}}\frac{1}{\sqrt{j\omega}}\right), & \text{for } \omega > \omega_s. \end{cases} \tag{32}$$

The transient admittance $y_o(t)$ is then given by $y_o(t) = Y_{LC}(\delta(t)+\tilde{y}(t))$, where $\tilde{y}(t)$ is such that $\tilde{y}(t) \to -\frac{R_o v}{\sqrt{2\pi}Z_{LC}}\frac{1}{\sqrt{t}}$, 0 for $t \to 0, \infty$ respectively. Since it must be $\int_o^\infty y_o(t)dt = 0$, consistently with $Y_o(0) = 0$, the compensation of the contribution of the δ-function depends on the area $A_y(t) = -\int_o^t \tilde{y}(t')dt'$, and as fas as $A_y \ll 1$ the $\tilde{y}$ term can be neglected[2]. We introduce a time scale t_y for which the $\tilde{y}$ term reduces the area of the δ-function by about 3% (*i.e.* $A_y(t_y) = -0.03$):

$$t_y \approx 10^{-3}\frac{\pi}{2}\left(\frac{Z_{LC}}{R_o v}\right)^2 = 10^{-3}\frac{Z_{LC}}{R_{DC}\mathcal{L}}\frac{\pi Z_{LC}}{2k_g v}\tau. \tag{33}$$

For very low-loss lines, when t_y is larger than the duration of the pulses of the transient, $y_o(t)$ can be effectively approximated by $Y_{LC}\delta(t)$.

APPENDIX III

For a scalar transmission line, the scattering parameters, defined with respect to a reference impedance Z_r, are

$$S_{11r} = S_R(Z_r, Z_o, H) = \frac{\mathcal{P}(Z_r, Z_o)(H^2-1)}{1-\mathcal{P}^2(Z_r, Z_o)H^2}$$
$$S_{21r} = S_T(Z_r, Z_o, H) = \frac{(1-\mathcal{P}^2(Z_r, Z_o))H}{1-\mathcal{P}^2(Z_r, Z_o)H^2} \tag{34}$$

with $\mathcal{P}(Z_r, Z_o) = \frac{Z_r - Z_o}{Z_r + Z_o}$. In low-loss lines, for which the bandwidth of $H(\omega)$ is larger than ω_s (see Appendix I), the choice $Z_r \neq Z_{LC}$ leads to multiple reflection resonances in the S_{pqr} functions.

APPENDIX IV

Signal propagation on the symmetric three-conductor structure of Fig. 3 can be represented in terms of an *even* and an *odd* mode, indicated by the subscripts e and o, respectively. The two modes are decoupled, and are described by the eigenvectors

$$\mathbf{u}_e = \frac{1}{\sqrt{2}}\begin{pmatrix}1\\1\end{pmatrix}, \qquad \mathbf{u}_o = \frac{1}{\sqrt{2}}\begin{pmatrix}1\\-1\end{pmatrix} \tag{35}$$

and by the propagation constants

$$K_i = \frac{\omega}{v_i}\sqrt{1 - j\frac{R_i(\omega)}{\omega L_i}}, \quad i = e, o \tag{36}$$

where $v_i = 1/\sqrt{L_i C_i}$, $R_{e,o} = R_{11} \pm R_{12}$, $L_{e,o} = L_{11} \pm L_{12}$, $C_{e,o} = C_{11} \pm C_{12}$, and R_{pq}, L_{pq}, C_{pq} are the elements of the line resistance, inductance and capacitance matrices, respectively [18]. The modal quantities $\mathbf{x}_m$ (*e.g.* voltages, or

[2]It must be $A_y(\infty) = 1$, for the exact compensation of the δ-function contribution.

currents, or voltage waves) are related to the corresponding physical quantities $\mathbf{x}$ by

$$\mathbf{x}_m = \begin{pmatrix} x_e \\ x_o \end{pmatrix} = \mathbf{E}^{\square}\mathbf{x} \tag{37}$$

where $\mathbf{E}^{\square} = \{\mathbf{u}_e, \mathbf{u}_o\}$ is the self-orthogonal matrix of the mode eigenvectors $\mathbf{u}_e$ and $\mathbf{u}_o$. Similarly, the modal matrix parameters $\mathbf{x}_m^{\square}$ (*e.g.* scattering or impedance matrices) are related to the corresponding physical quantities $\mathbf{x}^{\square}$ by $\mathbf{x}_m^{\square} = \mathbf{E}^{\square}\mathbf{x}^{\square}(\mathbf{E}^{\square})^{-1}$.

In the modal representation, the characteristic impedance is diagonal, *i.e.* $\mathbf{Z}_{om}^{\square} = \text{diag}\{Z_{oe}(\omega),\ Z_{oo}(\omega)\} = \text{diag}\{Z_{\text{LCe}} K_e \frac{v_e}{\omega},\ Z_{\text{LCo}} K_o \frac{v_o}{\omega}\}$, and the choice $\mathbf{Z}_r^{\square} = \mathbf{Z}_o^{\square}$ implies that $\mathbf{S}_{11rm}^{\square}$ is the null matrix and $\mathbf{S}_{21rm}^{\square} = \text{diag}\{H_e, H_o\} = \text{diag}\ \{\exp(-jK_e\mathcal{L}), \exp(-jK_o\mathcal{L})\}$, where H_e, H_o are the transmission transfer functions of the two modes.

ACKNOWLEDGMENT

We thank Professors M. Biey, V. Daniele, and G. Ghione for many helpful discussions and comments.

REFERENCES

[1] A. R. Djordjević, T. K. Sarkar, and R. F. Harrington, "Time-domain response of multiconductor transmission lines," *IEEE Proc.*, vol. 75, pp. 743–764, June 1987.
[2] A. J. Groudis and C. S. Chang, "Coupled lossy transmission line characterization and simulation," *IBM J. Res. Develop.*, vol. 35, pp. 25–41, 1981.
[3] A. R. Djordjević, T. K. Sarkar and R. F. Harrington, "Analysis of lossy transmission lines with arbitrary nonlinear terminal networks," *IEEE Trans. Microwave Theory Tech.*, vol. MTT-34, pp. 660–665, June 1986.
[4] J. E. Schutt-Aine and R. Mittra, "Scattering parameters transient analysis of transmission lines loaded with nonlinear terminations," *IEEE Trans. Microwave Theory Tech.*, vol. MTT-36, pp. 529–536, Mar. 1988.
[5] Q. Gu, Y. E. Yang, and J. A. Kong, "Transient analysis of frequency–dependent transmission line systems terminated on nonlinear loads," *Electrom. Waves and Applicat.*, vol. 3, pp. 183–197, Mar. 1989.
[6] F. Y. Chang, "Waveform relaxation analysis of nonuniform lossy transmission lines characterized with frequency-dependent parameters," *IEEE Trans. Circ. and Syst.*, vol. CAS-38, pp. 1484–1500, Dec. 1991.
[7] J. E. Schutt-Aine and R. Mittra, "Nonlinear transient analysis of coupled transmission lines," *IEEE Trans. Cir. and Syst.*, vol. CAS-36, pp. 959–967, July 1989.
[8] D. Winklestein, M. B. Steer, and R. Pomerleau, "Simulation of arbitrary transmission line networks with nonlinear terminations," *IEEE Trans. Circ. and Syst.*, vol. CAS-38, pp. 418–422, Apr. 1991.
[9] T. Komuro, "Time-domain analysis of lossy transmission lines with arbitrary terminal networks," *IEEE Trans. Circ. and Syst.*, vol. CAS-38, pp. 1160–1164, Oct. 1991.
[10] Q. Gu, D. M. Sheen, and S. M. Ali, "Analysis of transients in frequency–dependent interconnections and planar circuits with nonlinear loads," *IEE Proc.-H*, vol. 139, pp. 38–44, Feb. 1992.
[11] J. F. Mao and Z. F. Li, "Analysis of the time response of nonuniform multiconductor transmission lines with a method of equivalent cascaded network chain," *IEEE Trans. Microwave Theory Tech.*, vol. 40, pp. 948–954, May 1992.
[12] T. Dhaene and D. De Zutter, "CAD-oriented general circuit description of uniform coupled lossy dispersive waveguide structures," *IEEE Trans. Circ. and Syst.*, vol. 40, pp. 1545–1554, July 1992.
[13] R. E. Collin, *Foundations for Microwave Engineering*. New York: McGraw-Hill, 1992, ch. 4.
[14] A. Papoulis, *Signal Analysis*. New York: McGraw-Hill, 1977, ch. 7.
[15] A. Deutsch, G. V. Kopcsay, V. A. Ranieri, J. K. Cataldo, E. A. Galligan, W. S. Graham, R. P. McGouey, S. L. Nunes, J. R. Paraszczak, J. J. Ritsko, R. J. Serino, D. Y. Shih, and J. S. Wilczynski, "High-speed signal propagation on lossy transmission lines," *IBM J. Res. Develop.*, vol. 34, pp. 601–614, July 1990.
[16] J. R. Griffith and M. Nakhla, "Time-domain analysis of lossy coupled transmission lines," *IEEE Trans. Microwave Theory Tech.*, vol. 38, pp. 1480–1487, Oct. 1990.
[17] T. Hosono, "Numerical inversion of Laplace transform and some applications to wave optics," *Radio Sci.*, vol. 16, pp. 1015–1019, Nov. 1981.
[18] R. E. Matick, *Transmission Lines for Digital and Communications Networks*. New York: McGraw-Hill, 1969.
[19] C. R. Paul, *Introduction to Electromagnetic Compatibility*. New York: Wiley & Sons, Inc., 1992, chapter 4.

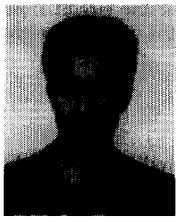

Ian Maio received the Laurea degree and the Ph.D. in electronic engineering from Politecnico di Torino, Turin, Italy, in 1985 and 1989, respectively.

Currently, he is with the Department of electronics at the Politecnico di Torino as a researcher. His research interests are in semiconductor lasers, distributed circuits and electromagnetic compatibility.

Sergio Pignari received the degree of Laurea in electronic engineering from the Polytechnic of Turin, Italy, in 1988.

He is currently a researcher with the Department of Electronics at the Polytechnic of Turin, Italy. His research interests are the electromagnetic compatibility and signal processing.

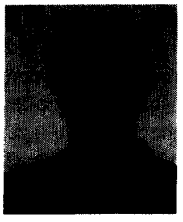

Flavio G. Canavero received the Laurea degree from the Politecnico di Torino, Turin, Italy, in 1977 and the Ph.D. degree from the Georgia Institute of Technology, Atlanta, GA, in 1986.

Currently, he is a Professor of Circuit Theory and Chairman of the Department of Electronics at the Polytechnic of Turin. His research interests are in the field of electromagnetic compatibility, where he works on the modelization of distributed electrical networks with linear and nonlinear loads, both from the point of view of the cross talk and susceptibility to external influences. Also, he studied the interaction of electromagnetic radiation with biological systems, and the remote sensing of the atmosphere.

He was the convener of the session on *Coupling to Mulitwire Cables* of the XXIV URSI General Assembly (Kyoto, 1993). He is a member of the Italian Electrotechnical and Electronic Association (AEI) and of the IEEE EMC Society.